Assessment of NDVI Composites Using Merged NOAA-14 and NOAA-15 AVHRR Data

Pei-yu Chen[1], Raghavan Srinivasan[1], Gunar Fedosejevs[2], Alma Delia Báez-González[3] and Peng Gong[4]

[1]Spatial Science Lab, Mail Stop # 2135, Department of Forest Science, Texas A&M University, College Station, Texas 77843, U.S.A.
[2]Canada Center for Remote Sensing, 588 Booth Street, Ottawa, Ontario, Canada, K1A 0Y7
[3]Laboratorio Nacional de Predicción de Cosechas y Monitoreo Climático, Campo Experimental de Pabellón, INIFAP, Km. 32.5 Carr. Zac-Ags., Ap. Postal #20, Pabellón de, Arteaga, Aguascalientes, Mexico
[4]Center for Assessment and Monitoring of Forest and Environmental Resources, Department of Environmental Science, Policy and Management, University of California, 151 Hilgard Hall, Berkeley, CA 94720-3110, U.S.A.

Abstract

The Advanced Very High Resolution Radiometer (AVHRR) data acquired by the National Oceanic and Atmospheric Administration's (NOAA) satellites provide daily observations of the Earth's surface. While NOAA-14 data from ascending orbits are operationally used for global vegetation monitoring; NOAA-15 data from descending orbits could provide additional daily coverage. The normalized difference vegetation index (NDVI), derived from the solar reflective data, is linked to vegetation condition and plant biomass production on land surfaces. Because a single AVHRR scene is seldom completely cloud-free, maximum value compositing (MVC) of multi-date NDVI data is widely used to minimize cloud contamination. While ten-day composites from NOAA-14 AVHRR data may not be cloud-free; critical short-term changes in vegetation condition may be lost in composites created over longer time periods. AVHRR data of Texas obtained from NOAA-15 (morning satellite) and NOAA-14 (afternoon satellite) were used in our study on the potential benefits of merged morning and afternoon NDVI data sets for crop monitoring. A strong correlation was observed between NOAA-14 and NOAA-15 NDVI data derived from top-of-atmosphere (TOA) reflectance.

I. INTRODUCTION

The National Oceanic and Atmospheric Administration (NOAA)-14 satellite was launched on December 30, 1994, and remains in operation today. Its main mission was to provide continuous coverage of Earth and global meteorological data by working as a companion satellite to NOAA-12 launched in 1991. NOAA-14 contains the Advanced Very High Resolution Radiometer/2 (AVHRR/2) as the primary imaging system. AVHRR/2 is a five-channel radiometer that is mainly used to map cloud cover and sea surface temperature. NOAA-15, launched on May 13, 1998, is expected to replace NOAA-12. The primary image system, AVHRR/3, onboard NOAA-15 was designed to get better measurements of atmospheric temperature and moisture values particularly under cloudy conditions. Compared to AVHRR/2 and earlier sensors, AVHRR/3 has six channels with only five active at any one time. An additional channel 3A is centered at 1.6 μm, and can be selected instead of the traditional channel 3B centered at 3.7 μm.

Many studies applying solar reflectance and normalized difference vegetation index (NDVI) derived from NOAA-AVHRR data require cloud-free data, because all cloud/smoke/haze/snow/ice contamination produces lower NDVI values. Unfortunately, a variety of cloud types are frequently observed in all AVHRR scenes. Maximum-value compositing (MVC) is widely used as a practical method to minimize the effects of cloud contamination (Holben, 1986). Texas is located next to the Gulf of Mexico, and thus clouds commonly extend from the southeast shore to central Texas. Few cloud-free scenes are available for creating weekly NDVI composites when data are collected from a single AVHRR sensor. Ten-day to bi-weekly NDVI composites built using only NOAA-14 AVHRR data may still be cloud-contaminated. An alternate approach to overcome cloud-contaminated composites is the use of post-processing of seasonal data developed by Cihlar (1996) or the use of post-composite cloud detection proposed by Gutman and Ignatov (1996); but these post-processing methods aren't possible for real-time delivery of composite data. AVHRR scenes of Texas are acquired by NOAA-15 in the morning and by NOAA-14 in the afternoon. Cloud cover usually increases through the day and cloud systems generally move across the sky. Thus, twice daily acquisition of AVHRR data is more likely to provide cloud-free coverage of areas of interest (Figure 1). Little has been published on NOAA-15 data processing and applications. The objective of this study was to assess the benefits of combining cloud-free NOAA-14 and NOAA-15 data to create NDVI composite coverage.

II. DATA SETS AND STUDY AREA

NOAA-15 AVHRR scan motor experienced an apparent failure between July 2000 and February 2001. High Resolution Picture Transmission (HRPT) images acquired from NOAA-15 were corrupted during this period of time. Most data for Texas acquired from NOAA-14 and -15 had solar zenith angles

1082-4006/02/0801-31 $5.00
©2002 The Association of Chinese Professionals in Geographic Information Systems (Abroad)

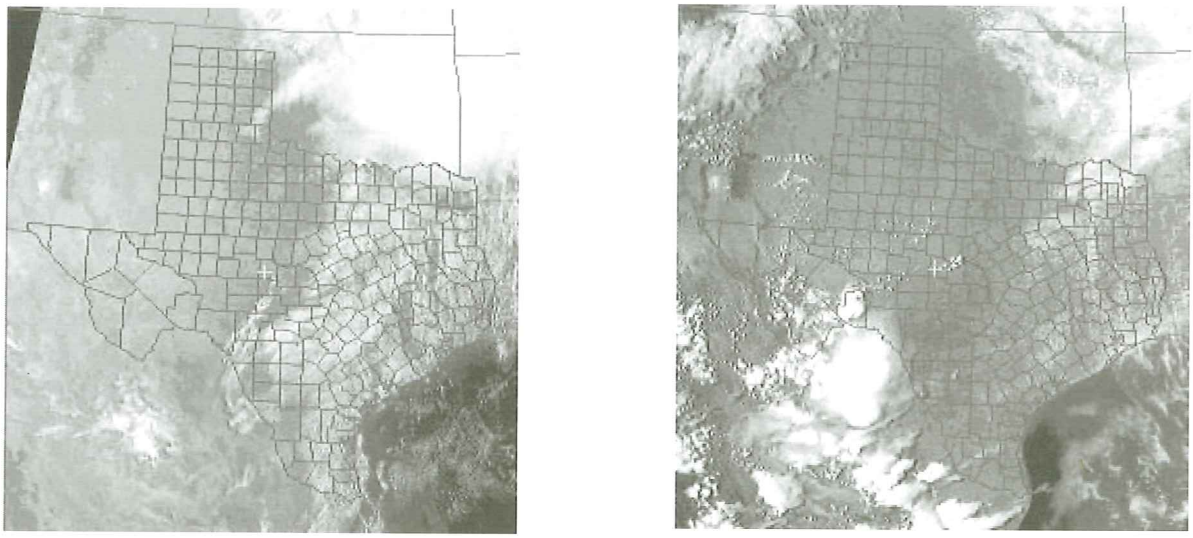

Figure 1. Geo-referenced AVHRR scenes of Texas downloaded from NOAA-15 (left) and NOAA-14 (right) on May 6, 2000

greater than 80° during the winter between November 1999 and February 2000. Both Holben (1986) and Singh (1988) suggested a limit of 80° for solar zenith angle for data applications. Due to data quality issues, AVHRR data sets for this study were limited to between March and June 2000, which is normally the start of the growing season in Texas.

Texas as the study site contains diverse land cover types. Eastern Texas is mainly dominated by a mixture of hardwood forests and pine plantations. Desert and barren land occupies most of western Texas except for Big Bend National Park. Northern Texas, also known as the Panhandle area, contains agricultural fields divided into segments, while southern Texas is dominated by rangeland. The densely populated urban areas are mostly located in central Texas. Since vegetation monitoring is one of the main applications for the data analyzed in this study, various vegetation cover types were selected based on 1992 classified LANDSAT Thematic Mapper (TM) images of the state of Texas created by the Blackland Research and Education Center in Temple, Texas (personal contact). The whole of Texas was classified into 9 classes: water, developed, barren, forested upland, shrubland, non-natural woody, herbaceous upland, herbaceous planted/cultivated, and wetlands. Each class was sub-divided into more detailed land cover types. For example, forest upland was sub-classified into deciduous forest, evergreen forest, and mixed forest. The vegetation types used for this study included rangeland, evergreen forest and deciduous forest.

III. METHODOLOGY

AVHRR HRPT data are downloaded daily from the NOAA-14 and -15 satellites to the receiving station located at the Texas A&M Blackland Research and Extension Center. The level 1b data products generated by Quorum software (Quorum Communications Inc., 1999) contain critical metadata required by users for radiometric calibration and geocoding. The metadata include orbit number, earth location in geographical coordinates, data acquisition time, thermal calibration data and other related information. The level 1b data were pre-processed using PCI image processing software (PCI Geomatic Group, 1998).

Piece-wise linear (PWL) calibration coefficients for NOAA-14 and NOAA-15 derived by Teillet and Fedosejevs (2001) at Canada Center for Remote Sensing (CCRS) were applied to the Texas data. The PWL coefficients were based on a post-launch calibration for NOAA-14 data. As post-launch calibration coefficients for NOAA-15 were not available, PWL coefficients based on pre-launch calibration were applied. The pre-processing for the two solar reflectance channels of NOAA-14 and -15 included radiometric calibration, reflectance conversion, atmospheric correction, bi-directional radiance distribution function (BRDF) correction, cloud removal, and computation of satellite zenith, solar zenith and relative azimuth angles. The set of atmospheric coefficients used to correct the NOAA-14 data were applied with the Simplified Method for Atmospheric Correction (SMAC) program (Rahman and Dedieu, 1994). A set of atmospheric coefficients to correct the NOAA-15 data was estimated based on spectral differences between NOAA-14 and -15 for use in this study. An automated cloud detection algorithm for NOAA-14 AVHRR data was applied for this study (Chen et al., 2002). No cloud detection algorithm was available for NOAA-15 data; thus, visual inspection was used to distinguish cloud-contaminated pixels from cloud-free pixels. All cloudy pixels detected by either an automated algorithm or visual inspection were discarded in this study.

Precipitable water vapor (PWV) content and aerosol optical depth (AOD) are two important inputs to SMAC. Since daily regional estimates of PWV and AOD were not available for Texas, nominal PWV (2.3 gm/cm^2) and AOD (0.05) values

were used in SMAC to correct the NOAA-14 and -15 data sets in this study. A BRDF correction developed by Latifovic at CCRS (personal communication) was applied to the NOAA-14 and -15 data. The BRDF correction coefficients were derived using all uncontaminated pixels separately for the different satellites and land cover types. Cihlar et al. (1997) implemented a BRDF correction that normalizes reflectance data in channels 1 and 2 to a satellite zenith angle of 0°, a solar zenith angle of 45°, and a relative azimuth angle of 0°. Solar reflectance and NDVI values were computed for the top-of-atmosphere (TOA), and at the surface before and after BRDF correction. The BRDF model applied in this study is given by:

$$\rho(\theta_s,\theta_v,\phi)=[1+(a_1+a_2*(1-\Delta)+a_3*(1-\Delta)^2)*f_1(\theta_s,\theta_v,\phi)+(a_4+a_5*\Delta+a_6*\Delta^2)*f_2(\theta_s,\theta_v,\phi)]*[1+a_7 e^{-\frac{\xi}{\pi}a_8}] \quad (1)$$

where, $a_1 - a_8$ are BRDF coefficients; θ_s is the solar zenith angle, θ_v is the satellite zenith angle, and ϕ is the relative azimuth angle; ρ_1 is the surface reflectance for the visible channel; ρ_2 is the surface reflectance for the near-infrared channel; $\Delta = NDVI$ for the visible channel; $\Delta = \rho_2 - \rho_1$ for the near-infrared channel;

$$\cos\xi = \cos\theta_s \cos\theta_v + \sin\theta_s \sin\theta_v \cos\phi\ ; \quad (2)$$

$$f_1(\theta_s,\theta_v,\phi) = \frac{1}{2\pi}[(\pi-\phi)\cos\phi + \sin\phi]\tan\theta_s \tan\theta_v - \frac{1}{\pi}(\tan\theta_s + \tan\theta_v + \sqrt{\tan^2\theta_s + \tan^2\theta_v - 2\tan\theta_s \tan\theta_v \cos\phi}) \quad (3)$$

$$f_2(\theta_s,\theta_v,\phi) = \frac{4}{3\pi} * \frac{1}{\cos\theta_s + \cos\theta_v}[(\frac{\pi}{2}-\xi)\cos\xi + \sin\xi] - \frac{1}{3} \quad (4)$$

AVHRR data received from NOAA-14 and -15 were applied to vegetation monitoring; thus, accurate geocoding of AVHRR data was very important in this study. Although AVHRR data were geocoded automatically using PCI software, manual checking and correction for each AVHRR scene was necessary to avoid extracting data from non-study sites. Overall, the maximum accuracy of geocoding for each scene was about 1 pixel or less, which meant that a target might be placed in any one of 9 pixels within a 3x3 window.

The 1992 classified Texas TM image was converted into grid data and then overlaid with AVHRR data in Albers Conical Equal-Area projection. A total of three regions (Figure 2) were selected as test sites from the daily NOAA-14 and -15 AVHRR scenes according to the classified TM images. They are mainly dominated by conifer forest, deciduous forest or rangeland. Eight uniformly distributed polygons were sampled in each selected region. Each polygon contained 121 pixels in a 11x11 window to minimize the effect of non-vegetated features. Eight polygons were selected to hopefully provide some cloud-free sample data for each scene, from which channel reflectance and NDVI seasonal profiles could be constructed.

Average satellite zenith, solar zenith and relative azimuth angles were computed for each polygon. The average reflectance and NDVI were computed from the eight polygons for each of the three study sites for a total of 24 polygon values. All of the daily reflectance and NDVI data available from both NOAA AVHRR sensors were used to analyze the correlation between NOAA-14 and NOAA-15 for each study region using linear regression. In addition, daily NDVI data from NOAA-14 and -15 were used to create NDVI composite values for each polygon based on the MVC procedure. Separate weekly maximum NDVI composite values for each polygon were produced from TOA reflectance and surface reflectance with and without BRDF correction.

IV. RESULTS AND DISCUSSION

An NDVI database of 24 polygon mean values (8 polygons for each land cover type) for each weekly composite period from March to June 2000 (17 weeks) and for each of the three NDVI product types was created in this study. None of the weekly NDVI composites had cloud-free data for all the polygons in any of the three test sites because of persistent cloud contamination. For a total of 17 NDVI values (17 weeks) for each polygon, most polygons had less than 10 NDVI values available for evergreen and deciduous forest sites, and had only three or four NDVI values available for the rangeland site. The cloud-free NDVI availability was averaged for each of the three land cover types (Table 1). The rangeland site close to the Gulf of Mexico had little NOAA-15 data because of water vapor contamination. Both the deciduous and evergreen forest sites were less influenced by clouds or water vapor.

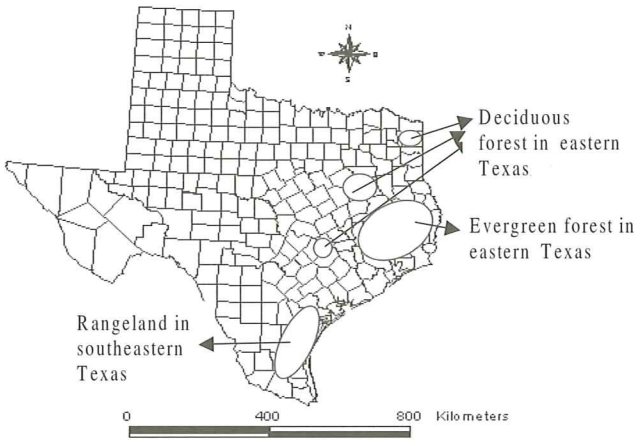

Figure 2. Study sites in Texas

Table 1. Average weeks of cloud-free NDVI availability out of the 17-week period

	Only morning data (NOAA-15) available	Only afternoon data (NOAA-14) available	Both data available	Both data unavailable
Deciduous	1.750	1.875	6.875	6.500
Evergreen	2.500	2.125	5.875	6.500
Rangeland	0.750	6.500	2.375	7.375

NOAA-15 reflectance

The NOAA-15 data were compared with the NOAA-14 data successfully used in real-time crop monitoring in Texas (Chen et al., in press) and early grain prediction in Mexico (Baez-Gonzalez et al., 2002). For several sorghum fields in Texas, temporal profiles of NDVI and field measured leaf area index (LAI) peak at the same time in irrigated fields. In addition, the NOAA-14 NDVI composites showed that it took three to four more weeks for sorghum to attain maximum NDVI in non-irrigated sites than in irrigated sites. This observation was validated with field data.

Daily cloud-free reflectance data (TOA and surface reflectance with and without BRDF correction) were combined according to satellite, channel and land cover type. Reflectance data were used in regression analysis only when both NOAA-14 and -15 data were available without cloud contamination on the same day. A low correlation was observed between NOAA-14 (afternoon orbits) and NOAA-15 (morning orbits) reflectance data for the same day, except for channel 2 in the rangeland area where an R^2 value of 71.25% was observed for the BRDF-corrected data (Table 2). The poor correlation between morning and afternoon data could be caused by sun-sensor geometry, solar intensity and different weather conditions between morning orbits and afternoon orbits in Texas. In addition, the use of default values for PWV and AOD might incur additional errors in the SMAC-corrected data. The correlations did improve for rangeland but not for deciduous and evergreen forests as would be expected after applying atmospheric and BRDF correction. However, the correlation results obtained from the rangeland site was not very reliable because of the small sample size. Moreover, very similar correlations between TOA and SMAC-corrected reflectance data were observed for both the visible and near-infrared channels. It is important to determine if the correlation between morning and afternoon reflectance data will be improved by applying real-time PWV and AOD values in the atmosphere correction.

Temporal profiles of visible and near-infrared reflectances were plotted for the data sets of deciduous forests (Figures 3 and 4). For the visible channel of NOAA-14 and -15, daily TOA reflectance data always had the highest values, and SMAC reflectance data had lower values. The results were different for the near-infrared channel, where TOA reflectance data had lower values than the SMAC-corrected reflectance data. The main reason for reflectance differences between TOA and SMAC-corrected data was that water vapor absorption and Rayleigh scattering strongly reduce measurements of the near-infrared channel (0.75-1.1μm) observed by the satellite sensors. The visible channel (0.58-0.68 μm) is weakly affected by ozone absorption (Ignatov and Stowe, 2002). As a result, the near-infrared reflectance data are more affected by atmospheric effects than visible reflectance observations. The near-infrared reflectances increased after atmospheric correction. The BRDF-corrected reflectance was consistently lower than the SMAC-corrected reflectance for the visible channel. Similar trends were not observed for the near-infrared channel. The BRDF correction varies not only with land cover type, but also with changes in phenology (with the maturation and senescence of vegetation), soil moisture content, and the optical and/or physical characteristics of the surface. In general, daily BRDF-corrected reflectance profiles were smoother (more so for the visible than the near-infrared channel) during the growing season compared to SMAC-corrected and TOA reflectance profiles. Visible reflectance profiles were smoother than the near-infrared reflectance profiles for the BRDF-corrected data. Moreover, NOAA-15 reflectance profiles were not as smooth as those for NOAA-14 data, but this could be attributed to morning solar variability (BRDF effects) of NOAA-15 data.

A couple of high values were observed for the April 20 and

Table 2. R^2 of linear regression between NOAA-14 and NOAA-15 reflectance data

	Number of Samples	Channel 1			Channel 2		
		TOA	SMAC	BRDF	TOA	SMAC	BRDF
Deciduous	43	0.02	0.02	0.12	0.04	0.05	0.05
Evergreen	45	0.02	0.00	0.09	0.28	0.28	0.18
Rangeland	16	0.03	0.14	0.29	0.36	0.37	0.71

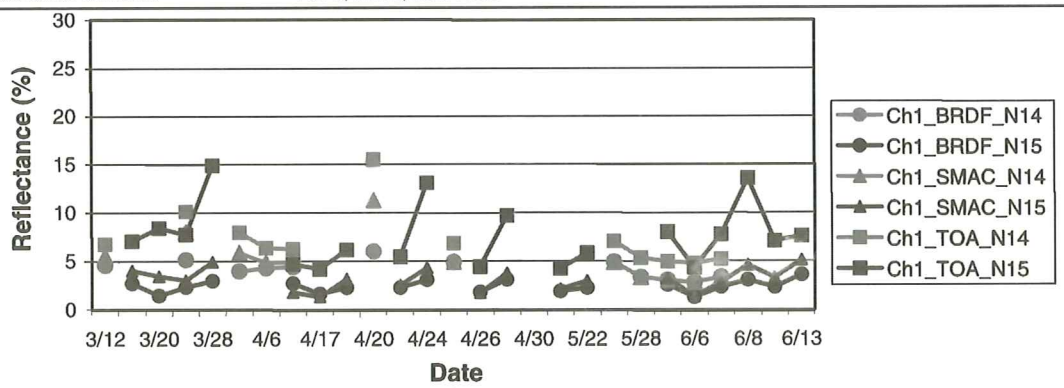

Figure 3. Temporal profile of visible reflectance of northeastern deciduous forest

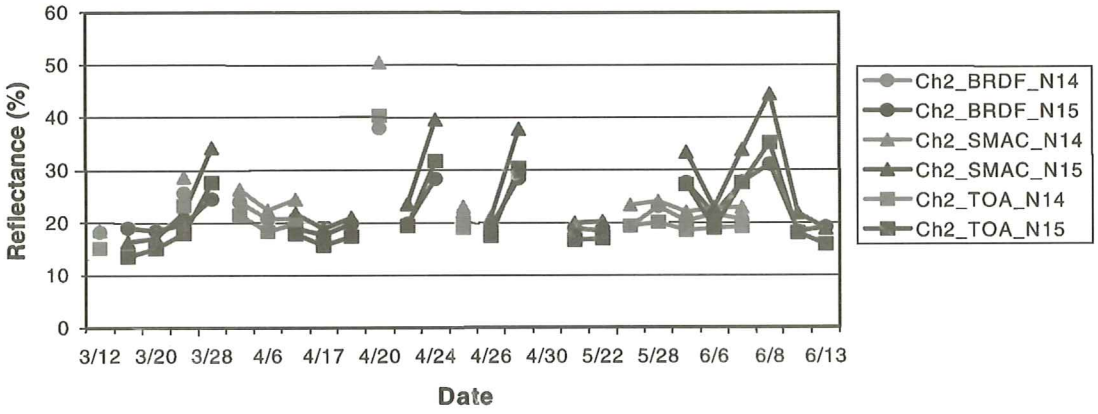

Figure 4. Temporal profile of near-infrared reflectance of northeastern deciduous forest

May 24 weekly composites for NOAA-14 BRDF-corrected reflectances in the near-infrared channel (Figure 4). The unusual reflectances were possibly produced by an inappropriate BRDF correction, because the faulty data had common characteristics, satellite zenith angle greater than 50° and solar zenith angle close to 60°. A similar situation happened for other data sets with high satellite and solar zenith angles. The BRDF model used for this study was developed for AVHRR data of high latitude areas such as Canada, where BRDF effects are more severe. Back scatter reflectance (where the sensor is positioned between the sun and target) was stronger than forward scatter reflectance (where the the sun is on the opposite side of the sensor) for the same location and time. The influence of BRDF might be lower in Texas, since Texas is located in a mid-latitude zone. More research in BRDF correction is necessary to improve AVHRR data accuracy and to derive local BRDF coefficients.

NOAA-14 vs. NOAA-15 NDVI

The idea of merging morning and afternoon NDVI data in composites was to acquire more cloud-free data. Although the correlation between NOAA-14 and NOAA-15 reflectance data was weak, the results for NDVI were more encourging. Schott (1997) mentioned that the use of NDVI can reduce atmospheric and illumination effects. Thus, NDVI data obtained from different satellites are supposed to have less influence by sun-sensor geometry, climate condition and solar intensity.

One polygon from each study region was selected for weekly NDVI composite plots (Figure 5). The three NDVI products NDVI-TOA, NDVI-SMAC and NDVI-BRDF were generated for each polygon based on TOA, SMAC-corrected and BRDF-corrected reflectance, respectively. The NDVI-TOA had the lowest values, and the NDVI-BRDF had the highest values. Although the NDVI-SMAC had higher values than the NDVI-TOA, both NDVI plots had very similar seasonal trends. Overall, the NOAA-15 NDVI-SMAC plots had fewer matches to the NOAA-14 NDVI-SMAC plots, which could be related to faulty estimates of atmospheric correction coefficients for NOAA-15 data. In addition, the behavior of NDVI-BRDF data was much different from that of NDVI-TOA and NDVI-SMAC, which could be caused by the use of improper BRDF coefficients. Hence, only the NDVI-TOA data were used for further analyses in our study.

NDVI-TOA seasonal profiles were generated separately from the NOAA-14 and -15 data for the three land cover types (rangeland, deciduous forest and coniferous forest). Results in Table 3 showed that both morning and afternoon NDVI had a higher correlation coefficient for the deciduous forest

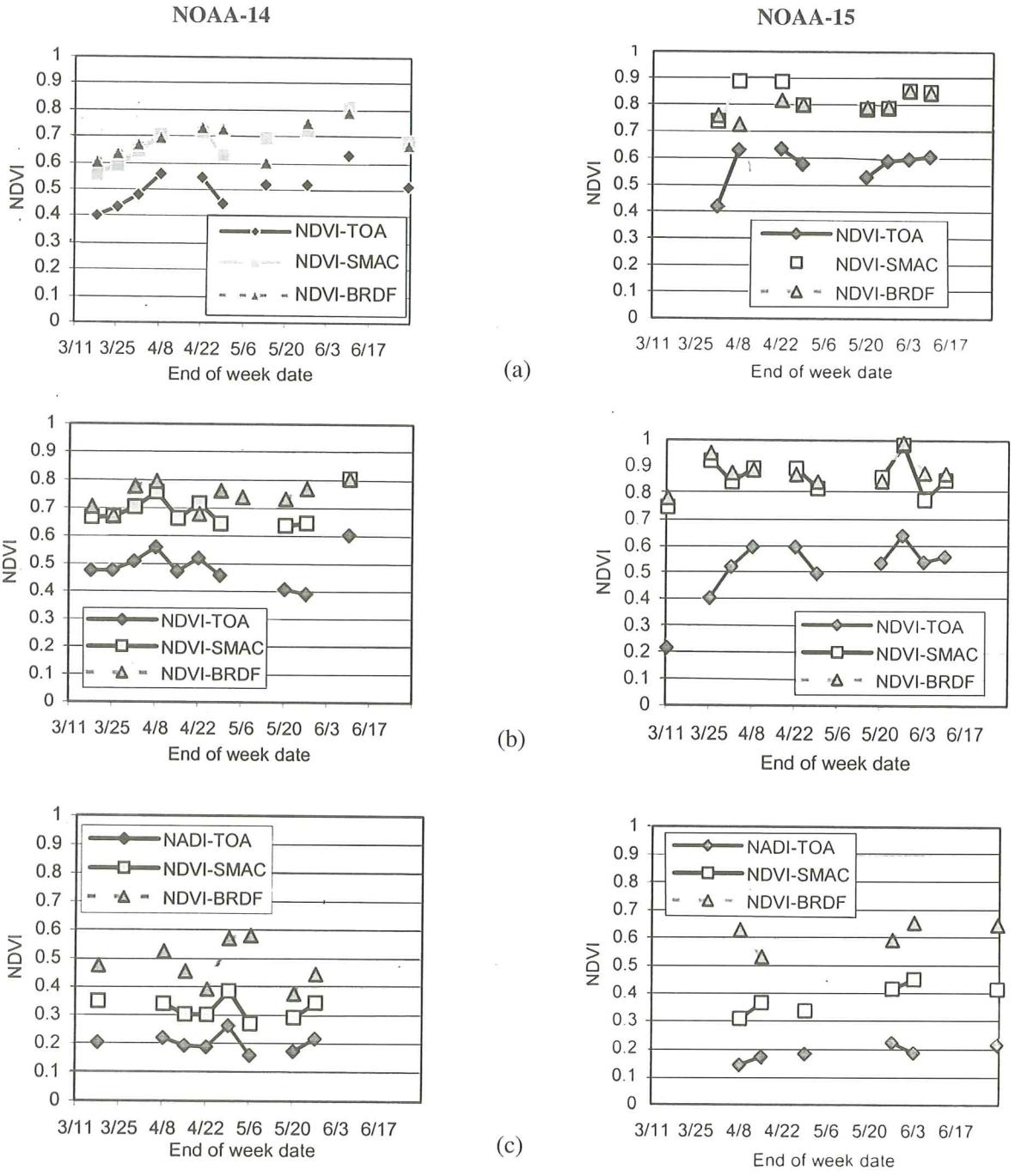

Figure 5. Weekly NDVI composites of (a) deciduous, (b) evergreen and (c) rangeland sites.

and rangeland study sites with R^2 values greater than 50%, but a lower correlation coefficient in the evergreen forest site. Lillesand and Kiefer (1994) mentioned that the NDVI is preferred over a simple ratio for global vegetation monitoring because NDVI helps compensate for changing illumination conditions, surface slope, aspect, and other extraneous features. Hence, the stronger correlation of morning and afternoon NDVI values was expected, though the linear relationship was poor for reflectance data. It was not clear why the evergreen forest had such a low NDVI correlation coefficient.

The NOAA-15 NDVI values were transformed based on the linear regression between NOAA-14 and NOAA-15 NDVI values, before both NOAA-14 and -15 data could be merged into the same composite. A study polygon was selected from the deciduous forest site for the linear regression transformation. Seasonal profiles were constructed from weekly NDVI composites using merged morning and afternoon NDVI values (Figure 6). The merged weekly NDVI composite values were anomalous for the weeks of May 27 and June 17, which could indicate that the vegetation was experiencing moisture stress. Overall, NOAA-15 AVHRR data provided

some extra cloud-free information that would otherwise not be available. Initial results from using merged NOAA-14 and NOAA-15 data sets for vegetation monitoring are encouraging. However, data correction and quality issues require further study. No attempt has been made here to address the issue of spectral adjustment factors to properly use NDVI values derived from multiple AVHRR data (Trishchenko et al., 2002).

Table 3. R^2 of linear regression between NOAA-14 and NOAA-15 NDVI data

	No. of Samples	R2
Deciduous	43	0.52
Evergreen	45	0.22
Rangeland	16	0.69

V. CONCLUSIONS

AVHRR data are critical to many operational products required in climate change and vegetation mapping studies. Accurate radiometric calibration of AVHRR sensor data is important for both time series analysis and inter-satellite comparisons. Post-launch calibration should be applied if possible, as is the case for NOAA-14. Because of the diverse range of illumination and viewing geometries observed in an AVHRR scene, atmospheric correction is important to properly compare pixels within a scene. It also helps to remove variable sky conditions when comparing scenes from different dates. The accuracy of atmospheric correction along with the calibration strongly affects the quality of the BRDF correction. More studies are required in the field of atmospheric and BRDF correction for AVHRR data to improve data quality. Our study also avoided the difficult issue of spectral adjustment factors. To properly compare spectral data from different satellites, the spectral response function of the channel has to be accounted for. Spectral adjustment factors are dependent on the target spectral reflectance and would need to be defined for every major land cover type, which was beyond the scope of this study. Trishchenko et al. (2002) have compiled generic spectral adjustment factors for NDVI derived from various NOAA AVHRR sensors with respect to NOAA-14 as the reference; but these were not available at the beginning of the study.

More NOAA satellites will be launched in the near future, which will provide more AVHRR data from different satellites. However, this will leave us with the challenge of merging data sets from the different AVHRR sensors for long-term studies. Since cloud contamination is an inevitable issue for AVHRR data users particularly around coastal areas, combining AVHRR data from different NOAA satellites can help overcome cloud problems during compositing of daily AVHRR scenes. Although poor correlation was observed between morning and afternoon reflectance data in this study, a relatively strong correlation existed for the NDVI-TOA data. As BRDF and atmospheric corrections are more problematic at large solar zenith angles, the potential application of merged morning and afternoon AVHRR data sets is likely limited to

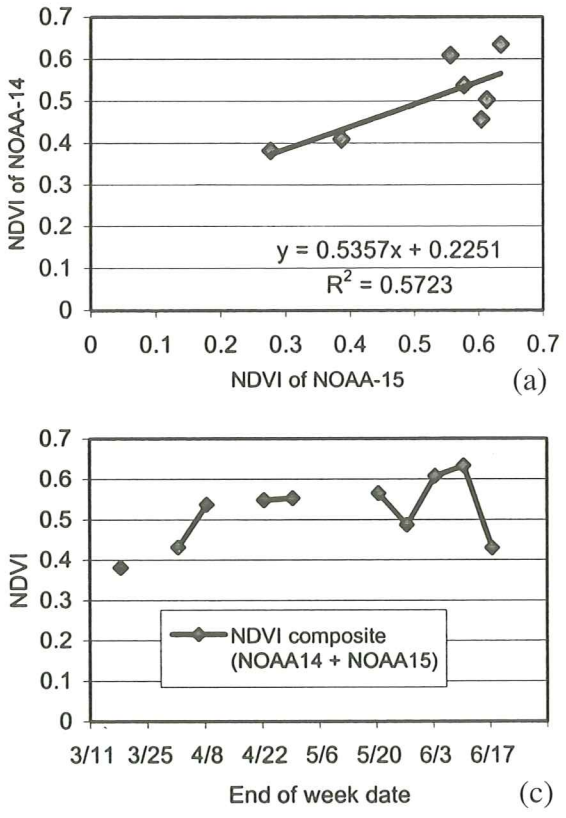

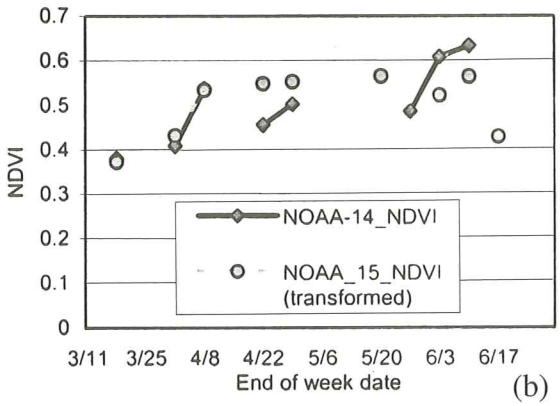

Figure 6. (a) Linear regression of weekly NOAA-14 and NOAA-15 NDVI, (b) weekly NOAA-14 vs. transformed NOAA-15 NDVI, and (c) weekly NDVI composites using merged NOAA-14 and NOAA-15 NDVI data

low latitude regions. More research is required to assess the potential benefits of merged data sets obtained from different NOAA satellites to vegetation monitoring in these regions.

ACKNOWLEDGEMENT

A portion of this research was supported by funds provided by the Texas Agricultural Experiment Station (TAES). The authors would like to thank Dr. Rasim Latifivic of Canada Center of Remote Sensing (CCRS) in Canada for the BRDF correction coefficients, Mr. Bill Park of CCRS in Canada for computer assistance, Dr. Robert Baker of the Department of Forest Science at Texas A&M University in U.S.A. for his many helpful comments, Quorum Communications in Canada for their technical support in using Qto1b software and PCI Geomatics Group in Canada for their technical assistance in using PCI software.

REFERENCES

[1] Baez-Gonzalez, A.D., P.Y. Chen, M. Tiscareño-Lopez, and R. Srinivasan, 2002, Satelite-based method of estimating corn yield in real time under irrigated and non-irrigated conditions in Mexico, *Crop Science*, 42(6).

[2] Chen, P.Y., R. Srinivasan, G. Fedosejevs, and J. Kiniry, accepted, Evaluating different NDVI composite techniques using NOAA-14 AVHRR data, *International Journal of Remote Sensing*, in press.

[3] Chen, P.Y., R. Srinivasan, G. Fedosejevs, and B. Narasimhan, 2002, An automated cloud detection method for daily NOAA-14 AVHRR data for Texas, U.S.A, *International Journal of Remote Sensing*, 23(15):2939-2950.

[4] Cihlar, J., 1996, Identification of contaminated pixels in AVHRR composite images for studies of land biosphere, *Remote Sensing of Environment*, 56(3):149-163.

[5] Cihlar, J., H. Ly, Z. Li, J. Chen, H. Pokrant, and F. Hunag, 1997, Multitemporal, multichannel AVHRR data sets for land biosphere studies: artifacts and corrections, *Remote Sensing of Environment*, 60(1):35-57.

[6] Gutman, G., and A. Ignatov, 1996, The relative merit of cloud/clear identification in the NOAA/NASA pathfinder AVHRR land 10-day composites. *International Journal of Remote Sensing*, 17(16):3295-3304.

[7] Holben, B.N., 1986, Characteristics of maximum values composite images from temporal AVHRR data, *International Journal of Remote Sensing*, 7(11):1417-1434.

[8] Ignatov, A., and L. Stowe, 2002, Aerosol retrievals from individual AVHRR channels. Part I: Retrieval algorithm and transition from Dave to 6S radiative transfer model, *Journal of the Atmospheric Sciences*, 59(3):313-334.

[9] Lillesand, T.M., and R.W. Kiefer, 1994, *Remote Sensing and Image Interpretation*, 3rd, John Wiley & Sons, Inc., New York, New York, 750p.

[10] PCI Geomatics Group, 1998, *Introduction to using PCI software*, version 7.0, PCI Enterprises, Richmond Hill, Ontario, Canada.

[11] Quorum Communications Inc., 1999, HRPT data capture engine, URL: *http://www.qcom.com/hrpt.html/*.

[12] Rahman, H., and G. Dedieu, 1994, SMAC: a simplified method for the atmospheric correction of satellite measurements in the solar spectrum, *International Journal of Remote Sensing*, 15(1):123-143.

[13] Schott, J.R., 1997, *Remote Sensing: The Image Chain Approach*, Oxford Unviersity Press, Inc., New York, New York, 394p.

[14] Singh, S.M., 1988, Simulation of solar zenith angle effect on global vegetation index (GVI) data, *International Journal of Remote Sensing*, 9(2):237-248.

[15] Teillet, P., and G. Fedosejevs, 2001, *Status of Radiometric Calibration for the NOAA-14/NOAA-15 Advanced Very High Resolution Radiometer (AVHRR)*, CCRS technical developments, URL: http://www.ccrs.nrcan.gc.ca/ccrs/tekrd/rd/ana/calval/.

[16] Trishchenko, A.P., J. Cihlar, and Z. Li, 2002, Effects of spectral response function on the surface reflectance and NDVI measured with moderate resolution sensors, *Remote Sensing of Environment*, 80:1-18.